RSC Advances

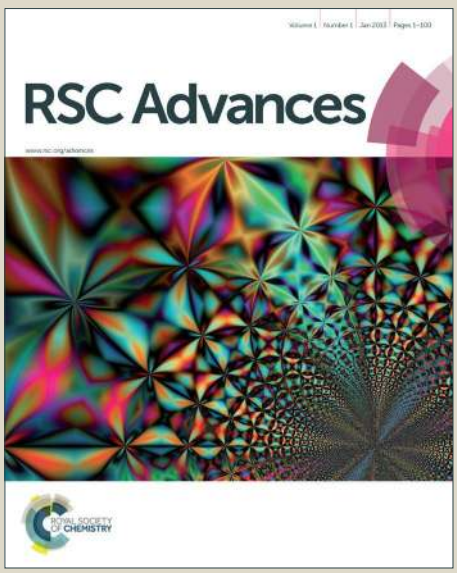

ROYAL SOCIETY OF CHEMISTRY

www.rsc.org/advances

View Article Online
DOI: 10.1039/C6RA20580A

A non-covalent interaction of Schiff base copper alanine complex with green synthesized reduced graphene oxide for highly selective electrochemical detection of nitrite

Subramanian Sakthinathan[a], Subbiramaniyan Kubendhiran[a], Shen-Ming Chen*[ac], Fahad M.A. Al-Hemaid[c], Wei Cheng Liao[a], P.Tamizhdurai[b], S. Sivashankar*[b], M. AjmalAli[c], A.A. Hatamleh[c]

[a]*Electroanalysis and Bioelectrochemistry Lab, Department of Chemical Engineering and Biotechnology, National Taipei University of Technology, No.1, Section 3, Chung-Hsiao East Road, Taipei 106, Taiwan (R.O.C).*

[b]*National Centre for Catalysis Research, Indian Institute of Technology, Chennai-600036, India.*

[c]*Department of Botany and Microbiology, College of Science, King Saud University, Riyadh 11451, Saudi Arabia*

Corresponding Author

[a]*(S.M. Chen). Fax: +886 2270 25238; Tel: +886 2270 17147*

E-mail address: smchen78@ms15.hinet.net

[b]*(S. Sivashankar) NCCR, IIT, Chennai.*

E-mail address: ssivasanker@iitm.ac.in

View Article Online
DOI: 10.1039/C6RA20580A

Abstract

A novel and selective nitrite sensor based on non-covalent interaction of Schiff base copper complex [Cu(sal-ala)(phen)] with reduced graphene oxide (RGO) was developed by simple eco-friendly approach. The morphology of the prepared RGO/[Cu(sal-ala)(phen)] nanocomposite was characterized by scanning electron microscopy (SEM), ultraviolet visible spectroscopy (UV), electro chemical impedance spectroscopy (EIS), energy dispersive x-ray spectroscopy, x-ray diffraction studies and Fourier transform infrared spectroscopy (FT-IR). On the other hand, the electrochemical studies of the prepared nanocomposite was investigated by cyclic voltammetry (CV) and amperometric technique. The RGO/[Cu(sal-ala)(phen)] nanocomposite modified glassy carbon electrode (GCE) exhibit the higher electrocatalytic activity towards detection of nitrite. Moreover, the RGO/[Cu(sal-ala)(phen)] modified GCE was determined the nitrite with low detection limit (19 nM), broad linear range (0.05-1000 μM) and high sensitivity (3.86 μA/μM cm^{-2}). Besides, the proposed sensor shows a good selectivity, repeatability, reprod ucibility and long term operational stability. The appreciable recoveries was achieved for the detection of nitrite in water and sausage samples, which implying that the practical feasibility of the modified electrode.

Keywords

Reduced graphene oxide, Schiff base copper complex, Nitrite, Green synthesis, Oxidation, Electrocatalysis, Sensitivity, Selectivity.

View Article Online
DOI: 10.1039/C6RA20580A

1. Introduction

Nitrites is an inorganic compound and it is widely used in food additives, corrosion inhibitors and fertilizing agents.[1-2] It can easily contaminated the drinking water due to the human activities, industrial pollutants and fertilizing agents.[3] The maximum permissible level of nitrite in drinking water is 1 mg/L and the excess of nitrite can causes several health problems like blue baby syndrome and shortness of breath. Moreover, nitrite can readily react with hemoglobin to form methemoglobin, which makes the oxygen deficiency in blood.[4,5] Besides, nitrite can react with various amines to the formation of N-nitrosamines and it causes stomach cancer to human. Therefore, it is very important to determination of nitrite in food, drinking water and environmental samples.[6] Nowadays, several analytical methods have been developed for the detection of nitrite including, chromatographic methods[7], capillary electrophoresis,[8] chemiluminescence[9], ion exchange chromatographic[10] and electrochemical methods.[11] Compared with other traditional analytical methods, electrochemical methods are widely used for the detection of nitrite due to the high sensitivity, simplicity and selectivity.[12,13] The unmodified electrodes are active towards detection of nitrite. However, the working potential was higher and selectivity also poor in the presence of interfering compounds. Hence, the chemically modified electrodes were used for the detection of nitrite due to the lowest oxidation potential and higher sensitivity.

Graphene is a two dimensional hexagonal carbon lattice with sp^2 hybridization. It has a wide spread applications because of its unique physicochemical properties such as high surface area, chemical stability, high electrical conductivity and extraordinary mechanical properties.[14,15] Comparatively, RGO has superior conductivity than GO due to the more active edge plane defects and large effective surface area,[16] so we need to find a suitable methods for reducing GO. Nowadays, different kinds of methods have been used for the preparation of RGO, which includes chemical vapor deposition (CVD),[17] mechanical exfoliation,[18] electric arc discharge,[19] thermal reduction[20] and chemical reduction.[21] Among all methods, the chemical reduction is more suitable and versatile method for the preparation of RGO in bulk quantities. However, in this method toxic and explosive chemicals are used for the RGO preparation. Therefore, we need to explore environmentally friendly reducing agents for effective reduction of GO.[22] Incidentally, the caffeic acid provides the good platform to the reduction of GO, because the caffeic acid (CA)

View Article Online
DOI: 10.1039/C6RA20580A

is one of the hydroxyl cinnamic acids and it has well antioxidant properties. Moreover, the structure of CA has two adjacent hydroxyl groups an aromatic ring, which helps donation of hydrogen to the GO reduction. Therefore, CA considered as a green, effective and low cost reducing agent for the RGO preparation.[23]

Schiff base complexes have an azomethine group (−HC=N−) that plays an important role in co-ordination chemistry. The Schiff bases are used to form stable complexes with transition metal ions. In addition, the Schiff base complexes are functionalized with RGO and used for different kinds of applications like sensors, catalysis and energy storage applications. [24-26] Besides, the non-covalent functionalization has advantages than covalent functionalization, because it avoids the destruction and retaining the unique properties of graphene. Moreover, the non-covalent interaction was enhanced the mechanical and electrical properties of the nanocomposite. [27, 28] In this work we have synthesized the RGO/[Cu(sal-ala)phen] (sal-ala = salicylalanine-alanine, phen =1, 10– phenanthroline) nanocomposite by non-covalent interaction. To the best of our knowledge for the first time Schiff base copper complex [Cu(sal–ala)phen] noncovalent interaction with RGO to prepare a new type of nanocomposite for the electrochemical detection of nitrite.

2. Experimental

2.1 Reagent and solution

Graphite powder (size < 20 μm), sodium nitrite, caffeic acid, L-alanine were purchased from sigma aldrich. 1, 10-phenanthroline, copper (II) chloride monohydrate and salicylaldehyde were purchased from Merck chemical. The phosphate (0.05 M) buffer solution (PBS) was prepared by using Na_2HPO_4 and NaH_2PO_4, the pH was adjusted by H_2SO_4 or NaOH. All the chemicals used in this work were of analytical grade and used without any further purification. Prior to each experiment, the electrolyte solutions were deoxygenated with purified N_2 for 15 min. All the experiment was carried out at room temperature and all the required solutions were made up by double distilled water.

2.2 Experimental apparatus

View Article Online
DOI: 10.1039/C6RA20580A

Electrochemical studies were carried out at the CHI 410 electrochemical work station. The electrochemical cell contains GCE as a working electrode, Ag/AgCl as a reference electrode and Pt wire as a counter electrode. The electrochemical experiment was performed at N_2 saturated electrolyte. UV-visible spectra were taken by Perkinelmer and electrochemical impedance spectra were carried out by the EIM6EX ZAHNER, Kroanch, Germany. Scanning electron microscope studies were carried out using a Hitachi S-3000H microscope. Elemental analysis was carried out using HORIBA EMAX X-ACT (model 51-ADD0009). Powder X-ray diffraction (XRD) studies were performed XPERT-PRO (Netherlands) diffractometer using Cu Kα radiation (k=1.54 Å). Fourier transform infrared spectroscopy (FT-IR) was carried out using the Jasco FT-IR 6600 spectrometer.

2.3 Preparation of [Cu (sal-ala)(phen)] complex

The inorganic complex was synthesized based on previous report with slight modification.[29-32] 1,10-phenanthroline (5 mmol; 0.99 g in 20 mL methanol) and salicylalanine (5 mmol; 0.97 g in 20 mL methanol) ligands were mixed and homogenized. Then the homogenized solution was added dropwise to a solution of $CuCl_2.H_2O$ (5 mmol; 0.86 g in 20 mL water) while stirring at 50 °C. The bright green precipitate of [Cu(sal-ala)(phen)] complex was obtained (scheme 1), this precipitate was filtered and washed with ethanol then dried in a desiccator. The prepared Schiff base complex was confirmed by the UV visible and FT-IR spectroscopy.

2.4 Preparation of RGO/[Cu(sal-ala)(phen)] inorganic nanocomposite

Graphene oxide was prepared from graphite by modified hummers method.[33] The RGO was prepared by the following procedure of Bo *et al* method.[34] 10 mg of GO was dispersed in 100 mL deionized water and caffeic acid (CA) (5 mg) was added in to the GO dispersion. The mixture was then heated at 95° C for 24 hours in an oil bath with the assistance of stirring. The resulting suspension was collected and washed with deionized water and ethanol. Finally, the prepared RGO was dried at 35° C under vacuum condition.

The non-covalent approach was used to prepare the RGO/[Cu(sal-ala)(phen)] nanocomposite with distinctive electrocatalytic activity towards the oxidation of nitrite.[35] The nanocomposite was synthesized by dispersing the RGO in DMF and further addition of [Cu(sal-ala)(phen)] under vigorous stirring. Then, the obtained homogeneous solution was subjected to ultrasonic

View Article Online
DOI: 10.1039/C6RA20580A

treatment (30 min) for enhancing the interaction between RGO and [Cu(sal-ala)(phen)]. The resultant homogeneous RGO/[Cu(sal-ala)(phen)] nanocomposite was filtered and washed with ethanol three times and dried in oven. Finally, the prepared RGO/[Cu(sal-ala)(phen)] was re-dispersed in DMF (1 mL) and drop casted on the cleaned GCE surface then dried in room temperature. The scheme 2 displays the preparation of GCE/RGO/[Cu(sal-ala)(phen)] modified electrode for the electrochemical detection of nitrite.

3. Result and discussion

3.1 characterization of prepared nanocomposite

Fig 1 shows the SEM images of (A) GO, (B) RGO, (C) GO/[Cu(sal-ala)(phen)], (C') [Cu(sal-ala)(phen)], (D) RGO/[Cu(sal-ala)(phen)]. The SEM image of graphene oxide shows the thin and wrinkled surface. In addition, RGO exhibited randomly aggregated with distinct edges and folding sheet surfaces. The SEM image of GO/[Cu(sal-ala)(phen)] exhibit the Schiff base copper complex incorporated on the GO surface and the inset Fig C' shows the SEM image of [Cu(sal-ala)(phen)] complex. The SEM image of RGO/[Cu(sal-ala)(phen)] nanocomposite can be observed that the [Cu(sal-ala)(phen)] inorganic complex was uniformly covered on the RGO surface. Furthermore, the elemental composition of as-prepared nanocomposite was explored by elemental analysis. Fig 1E and F displayed the EDX spectra of RGO/[Cu(sal-ala)(phen)] nanocomposite. Where, the signals for carbon, oxygen, nitrogen and copper confirmed the formation of nanocomposite. Notably, the signals of copper and nitrogen confirms the Schiff base formation and complexation.

EIS has been used to understand the charge transfer resistance (R_{ct}) of the different modified electrodes at the electrode and electrolyte interface. Fig 2A shows the EIS plots of (a) bare GCE, (b) GCE/RGO, (c) GCE/[Cu(sal-ala)(phen)], (d) GCE/GO/[Cu(sal-ala)(phen)], (e) GCE/RGO/[Cu(sal-ala)(phen)] in 5 mM $[Fe(CN)_6]^{3-/4-}$ with 0.1 M KCl as a supporting electrolyte. The diameter of the semicircle is corresponding to the charge transfer resistance (R_{ct}) of the modified electrodes. The higher R_{ct} value of about 1561 Ω was observed for the GCE/[Cu(sal-ala)(phen)] modified electrode. The bare GCE and GCE/RGO shows the R_{ct} value of 378 Ω and 244 Ω respectively. However, the R_{ct} value of GCE/GO/[Cu(sal-ala)(phen)] modified electrode observed about 235 Ω, the charge transfer resistance of Schiff base copper complex was

View Article Online
DOI: 10.1039/C6RA20580A

decreased due to the non-covalent interaction with GO. Interestingly, the GCE/RGO/[Cu(sal-ala)(phen)] modified electrode shows the low R_{ct} value of 33 Ω due to the reduction of GO to RGO, which enhance the conductivity of the modified electrode. The EIS results confirmed that the GCE/RGO/[Cu(sal-ala)(phen)] modified electrode have higher electron transfer properties with low charge transfer resistance. The UV-Visible spectra was used to identify the structural information about the nanocomposites. Fig 2B shows the UV visible spectra of (a) RGO, (b) [Cu(sal-ala)(phen)] and (c) RGO/[Cu(sal-ala)(phen)]. The synthesized RGO shows the absorbance peak at 283 nm, it confirms that the GO was successfully reduced by CA with the eco-friendly route. Furthermore, the absorbance peak at 222 nm for the π-π* transition of phenanthroline and 272 nm for n-π* transition of the salicylidene. The Cu (II) complex exhibited the UV visible spectra at 372 nm due to the ligand to metal charge transfer transition and the RGO/[Cu(sal-ala)(phen)] shows the peaks that observed in the free base confirms the formation of nanocomposite.[36]

The Fig 3A shows the X-ray diffraction studies of (a) RGO, (b) [Cu(sal-ala)(phen)], (c) RGO/[Cu(sal-ala)(phen)]. The XRD pattern of RGO shows the broad peak at 26° due to the short range order for stacked layer. On the other hand, the XRD spectra of [Cu(sal-ala)(phen)] shows the peaks at 11º, 12.6º, 17º, 19º, 22º and 25º. Which confirms the formation of schiff base copper (II) complex. Besides, the XRD spectra of RGO/[Cu(sal-ala)(phen)] observed at 11°, 12°, 25°, 30°, 41° and 69° are quite similar to the [Cu(sal-ala)(phen)].[37] However, the intensity has fall down and the peak shapes are changed. This results confirmed that the formation of RGO/[Cu(sal-ala)(phen)] nanocomposite. The surface chemistry, bonding nature and chemical structure of the prepared nanocomposite was characterized by FT-IR spectra**.** Fig 3B shows the FT-IR spectra of (a) RGO, (b) [Cu(sal-ala)(phen)], (c) RGO/[Cu(sal-ala)(phen)]. The FT-IR spectrum of RGO exhibited the characteristic peak at 3452 cm^{-1} for the stretching vibration of hydroxyl groups. Moreover, the peaks observed at 1725 cm^{-1} and 1229 cm^{-1} are corresponding to the stretching vibration of C=O and C-O. The stretching vibration peak appeared at 833 cm^{-1} for the C-H rocking vibration which confirms the phenanthroline functionalities in [Cu(sal-ala)(phen)]. The peak in the region of 2063 cm^{-1} for N-H bonds of Schiff-base complex. The Cu-O band appeared at 930 cm^{-1} and Cu-N appeared at 528– 549 cm^{-1}. The peak at around 2918 cm^{-1} and 2892 cm^{-1} can be assigned to C–H and CH_2 stretching vibration respectively. The FT-IR spectra of RGO/[Cu(sal-ala)(phen)] nanocomposite shows the stretching vibration similar to

View Article Online
DOI: 10.1039/C6RA20580A

the RGO and [Cu(sal-ala)(phen)].[33] The FT-IR results confirmed that the Schiff base copper complex has been non-covalently interact with RGO and leads to the composite formation.

4. Electrocatalytic oxidation of nitrite

4.1 Electrocatalytic oxidation of nitrite at various modified electrodes and effect of different concentration

Fig 4A shows the CV curves of (a) RGO/[Cu(sal-ala)(phen)] nanocomposite modified electrode in the absence of nitrite and (b) bare GCE, (c) GO, (d) [Cu(sal-ala)(phen)], (e) RGO, (f) GO/[Cu(sal-ala)(phen)], (g) RGO/[Cu(sal-ala)(phen)] nanocomposite modified electrodes in the presence of 200 μM nitrite in PBS (pH 5). The bare GCE and GO modified electrodes oxidize the nitrite at the peak potential (E_P) of 0.99 V and 0.98 V with a corresponding oxidization peak current of (I_P) 25.23 μA and 27.38 μA respectively. In addition, the [Cu(sal-ala)(phen)] modified electrode displays the E_P and I_P of about 1.056 V and 30.64 μA. Besides, the RGO modified electrode exhibits the E_P of 0.964 V and the I_P of 31.33 μA for the oxidation of nitrite. Furthermore, the GO/[Cu(sal-ala)(phen)] modified electrode shows the value of E_P and I_P at 0.93 V and 43.9 μA respectively for the oxidation of nitrite. Comparatively the oxidation peak current of nitrite was increased for GO/[Cu(sal-ala)(phen)] modified electrode than that of [Cu(sal-ala)(phen)] and RGO modified electrodes. These results confirmed that the formation of non-covalent interaction between the GO and [Cu(sal-ala)(phen)], which enhanced the catalytic activity. Generally, the RGO shows the better electrocatalytic properties than GO because the GO contains many oxygen functionalities, which creates an internal resistance at the modified electrode. In this aspect, the RGO/[Cu(sal-ala) (phen)] nanocomposite was prepared and applied for the determination of nitrite alternative to the GO/[Cu(sal-ala)(phen)]. As expected, the RGO/[Cu(sal-ala)(phen)] nano composite exhibits the substantial oxidization peak potential at (E_P) 0.97 with an improved oxidation peak current (I_P) of 49.80 μA, which are comparatively higher than that of all aforementioned modified electrodes. These results can be attributed to the non-covalent interaction of RGO and [Cu (sal-ala) (phen)], which plays an important role in the oxidation of nitrite due to their extraordinary electro catalytic activity. Hence, the RGO/[Cu(sal-ala)(phen)] nanocomposite modified electrode as an excellent electrode material for nitrite sensor. Fig 4B shows the CV curves of RGO/[Cu(sal-ala)(phen)] nanocomposite modified electrode for the oxidation of nitrite in various concentrations of nitrite containing PBS (pH 5) at

View Article Online
DOI: 10.1039/C6RA20580A

the scan rate 50 mVs^{-1}. Increasing the concentration of nitrite from 50 µM to 600 µM, the oxidized peak current also increased linearly. The Fig 4B inset shows the linear relation between the peak current vs concentration and the corresponding linear regression equation can be expressed as I_{pa} =0.5074x - 40.813 with a correlation coefficient R^2 =0. 9947. It is evident that the RGO/[Cu(Sal-ala)(phen)] nanocomposite modified GCE electrode has the good electrocatalytic activity towards the detection of nitrite.

4.2 Effect of pH and scan rate

The influence of pH in the performance of an as-prepared modified electrode was investigated for the detection nitrite using CV. The CV experiment was recorded at RGO/[Cu(sal-ala)(phen)] modified GCE in various pHs ranging from 1 to 9 towards the electrocatalytic oxidation of 200 µM nitrite. As shown in the Fig 5A, the oxidation peak current of the nitrite was increased when increasing the electrolyte pH from 1 to 5 afterwards it decreases by varying the pH 6 to 9. This result stated that, at lower pH the NO_2^- ions are unstable so it can be easily converted to NO and NO_3^-. At the same time in higher pHs, the proton deficiency was occurred. However, at pH 5 the sensor exhibited higher electro catalytic performance (Fig 5B). Therefore, we have choose pH 5 for further electrochemical studies. Fig 6A shows the typical CV curve obtained at the RGO/[Cu(sal-ala)(phen)] modified electrode for the different scan rates in PBS (pH 5) containing 200 µM nitrite. The result showed that the peak current was linearly increased with respect to the increasing scan rates from 0.01 to 0.11 Vs^{-1}. Fig 6B shows corresponding plot of peak current (I_p) Vs square root of scan rate ($v^{1/2}$) and calculated the corresponding linear regression equation as $I_p = 75.58\ v^{1/2}\ (Vs^{-1})^{1/2} + 10.60$ with $R^2 = 0.998$. From this result, we have concluded that the oxidation of nitrite is diffusion-controlled process at RGO/[Cu(sal-ala)(phen)].[38] Moreover, the electrocatalytic oxidation of nitrite at RGO/[Cu(sal-ala)(phen)] modified electrode is an irreversible process and the anodic peak shifted to positive potential when increasing the scan rate. The electron transfer co-efficient and the number of electrons transfer involved in the rate-determining step can be estimated by the following equations

$$E_{pa} = [2.303\ RT/2\ (1-\alpha)\ n_a\ F\ ]\ \log v + K \qquad (a)$$

$$I_p = (2.99 \times 10^5)_n\ [(1-\alpha)n_a]^{1/2}\ AC_0 \times D_0^{1/2}\ v^{1/2} \qquad (b)$$

View Article Online
DOI: 10.1039/C6RA20580A

Where K is a constant, n_a is 1 and substituting the slope of E_{pa} versus log v plot, in the equation (a) the value of α was obtained as 0.52 for the nitrite oxidation. Furthermore, the number of electrons involved in the oxidation of nitrite can be estimated by the equation (b) for totally irreversible process controlled by diffusion. For equation (b), the D_0 is the diffusion coefficient of nitrite, A is the electrode area and C_0 is the concentration of nitrite. By substituting all the values in the above equation (b), the value of n estimated to be 2. This result indicated that the nitrite oxidation lead to NO_3^- as a final product and it is good accordance with the literature. The overall nitrite oxidation reaction can expressed by the equation (c) and (d)

$$NO_2^- - e^- \rightarrow NO_2 \quad (c)$$

$$2NO_2 + H_2O \leftrightarrow NO_3^- + NO_2^- + 2H^+ \quad (d)$$

From these results, the electro catalytic oxidation of nitrite at the RGO/[Cu(sal-ala)(phen)] nano composite modified electrode as a two electron transfer reaction.[39]

4.3 Amperometric determination of nitrite

Fig 7A shows the amperometric response of RGO/[Cu(sal-ala)(phen)] nanocomposite modified rotating disc electrode (RDE) recorded at the rotation speed of 2000 rpm. The nitrite was successively added in PBS with 50 s interval for every additions under the convection mode with the applied working potential (E_{app}) of +0.85 V. Herein, a sharp amperometric signal was appeared for the determination of nitrite for the addition of 0.05 μM nitrite. Followed by that addition, the concentration of nitrite was increased to 1000 μM. The resultant oxidation peak current was linearly increased with increasing the concentration of nitrite (0.05 to 1000 μM). From this result, we have observed two linear concentration ranges such as 0.05 – 4 μM (low) and 6–1000 μM (high) for the determination of nitrite and the corresponding calibration plot was shown in Fig 7B and C, respectively. The sensitivity of the fabricated sensor was calculated to be 3.86 μA/μM cm^{-2} and the lowest detection limit (LOD) calculated about 19 nM. The sensitivity of the proposed sensor was compared with some other graphene based nitrite sensor. Notably, the RGO-MWCNT-Pt/Mb fabricated electrode was used for nitrite sensor with the sensitivity of 0.1651μA/μM/cm^{-2} and GNPs/MWCNT modified electrode exhibit the sensitivity of about 2.58 μA/μM cm^{-2}.[40,41] By the way, many of nitrite sensor electrodes were fabricated on the graphene derivatives.[42-44]However,the RGO/[Cu(sal-ala)(phen)] nanocomposite modified electrode have

View Article Online
DOI: 10.1039/C6RA20580A

exhibited the high sensitivity (3.86 μA/μM /cm^{-2}) than that of the previously reported nitrite sensor electrodes. Hence, it is evident that the Schiff base copper (II) complexes could be an effective electrocatalyst for the oxidation of nitrite due to the higher electron transfer rate and well redox properties. In addition, the high surface area of RGO provides strong interaction between RGO and [Cu(sal-ala)(phen)]. The RGO/[Cu(sal-ala)(phen)] nanocomposite exhibited the acceptable selectivity, wide linear range and low detection limit of nitrite. These observed analytical results are compared with several others nitrite sensor electrode tabulated as shown in Table 1.

4.4 Interference and real sample studies

We have analyzed the selectivity of RGO/[Cu(sal-ala)(phen)] nanocomposite modified electrode towards the detection of nitrite in the presence of common interference ions such as anions, cations and biological sample. The experimental condition was similar to in section 4.3 and the corresponding amperogram shown in Fig 8A. The RGO/[Cu(sal-ala)(phen)] modified electrode exhibited the well sharp amperometric response for the each 5 μM additions of nitrite (a). Whereas, there is no response appeared for the 500 μM additions of other interfering ions, such us (b) Br^-, (c) I^-, (d) Cl^-, (e) NO_3^-, (f) F^-, (g) Cu^{2+}, (h) Zn^{2+}, (i) Cr^{2+}, (j) Sr^{2+}, (k) K^+, (l) dopamine, (m) glucose, (n) fructose and (o) ascorbic acid. This study revealed that the RGO/[Cu(sal-ala)(phen)] fabricated electrode selectively detect the nitrite even in the presence of excess interfering compounds. Therefore, the RGO/[Cu(sal-ala)(phen)] nanocomposite applied to the detection of nitrite in real time monitoring application. The practical feasibility of the RGO/[Cu(sal-ala)(phen)] modified sensor has been demonstrated by amperometric method in various sources of water samples and sausage meat sample. The water sample were collected from the river and lake, the sausage sample was collected from local market in Taiwan. Before performing the real sample analysis the collected water sample was subjected to the filtration and remove the solid suspension. The standard addition method was used for the real sample analysis and the obtained recoveries are 93.5 %, 94.3 % and 94.2 % is shown in Table 2. This result endorsed that the developed nitrite sensor electrode has an acceptable recoveries in real sample analysis. Thus, the modified electrode can be used for the determination of nitrite detection in water and food samples.

View Article Online
DOI: 10.1039/C6RA20580A

4.5 Repeatability, reproducibility and stability studies of RGO/[Cu(sal-ala)(phen)] nanocomposite modified electrode

The repeatability and reproducibility of the proposed sensor was carried out by the CV studies in the presence of 200 μM nitrite in PBS (pH 5). The modified electrode was exhibited an acceptable repeatability with the RSD of about 3.55 % for the 10 repetitive measurements examined by the single modified electrode. Moreover, the fabricated sensor electrode shows the appreciable reproducibility of 3.45 % for the 10 measurements carried out by 10 different modified electrodes. The obtained results showed that the RGO/[Cu(sal-ala)(phen)] nanocomposite modified electrode have good repeatability and reproducibility. The storage stability of the fabricated electrode was investigated periodically in PBS containing 200 μM nitrite in an inert atmosphere. Fascinatingly, RGO/[Cu(sal-ala)(phen)] exhibited only 3.6 % of peak current changes from its initial peak current response after the 30 days storage. The operational stability of the RGO/[Cu(sal-ala)(phen)] nanocomposite modified electrode was carried out by the amperometric technique in the presence of 50 μM nitrite for 3000 s (Fig 8B). The experimental condition was similar as we discussed in the section 4.3 and manifest the oxidized peak current loss only 2.2 % from the initial current. The obtained results reveals the excellent operational stability and antifouling properties of the modified electrode.

5. Conclusions

In summary, we have successfully prepared a novel and stable RGO/[Cu(sal-ala)(phen)] nanocomposite via non-covalent interaction and the prepared nanocomposite was characterized by different microscopy and spectroscopic techniques. The RGO/[Cu(sal-ala)(phen)] nanocomposite modified electrode showed an excellent electrocatalytic activity towards detection of nitrite with wide linear concentration range (0.05-1000 μM), low detection limit (19 nM) and high sensitivity (3.86 μA/μM cm^{-2}). The modified electrode offered an appreciable repeatability and reproducibility. Moreover, the fabricated electrode was selectively determined the nitrite even in the presence of interfering ions and biological molecules. Moreover, the developed sensor electrode showed the good recoveries in real sample analysis from sausage meat and water samples. Therefore, we concluded that the RGO/[Cu(sal-ala)(phen)] nanocomposite modified electrode can be used as an excellent electrode material for the electrochemical detection of nitrite. This proposed sensor electrode can be used in future for the

View Article Online
DOI: 10.1039/C6RA20580A

accurate detection of nitrite in food and industrial samples. The reported Schiff base complex have an advantages in terms of easy way to prepare, stable complex formation and higher electrochemical activity. Thus, the Schiff base complex based nanomaterials have been extended to develop a new electrochemical sensor.

Acknowledgement

The authors extend their appreciation to the International Scientific Partnership Program ISPP at King Saud University for funding this research work through ISPP#6. Furthermore, this project was supported by the National science council & Ministry of science and technology of Taiwan (ROC).

View Article Online
DOI: 10.1039/C6RA20580A

References

[1] S. Palanisamy, B. Thirumalraj, S. M. Chen, *J. Electroanal. Chem*, 2016, **760**, 97.

[2] Y. Haldorai, J. Y. Kim, A. T. E. Vilian, N. S. Heo, Y. S. Huh, Y. K. Han, *Sens. Actuators, B*, 2016, **227**, 92.

[3]V. Mani, T. Y. Wu, S. M. Chen, *J. Solid State Electrochem*, 2014, **18**, 1015.

[4] A. Rahim, L. S. S. Santos, S. B. A. Barros, L. T. Kubota, R. Landers, Y. Gushikem. *Electroanalysis*, 2014, **26**, 1.

[5] J. P. Salome, R. Amutha, P. Jagannathan, J. J. M. Josiah, S. Berchmans, V. Yegnaraman, *Biosens. Bioelectron*, 2009, **24**, 3487.

[6] L. Cui, J. Zhu, X. Meng, H. Yin, X. Pan, S. Ai, *Sens. Actuators*, B, 2012, **161**, 641.

[7] A. Jain, R. M. Smith, K. K. Verma, *J. Chromatogr. A*, 1997, **760**, 319.

[8] E. V. Trushina, R. R. Oda, J. P. Landers, C. T. Mcmurray, *Electrophoresis*, 1997, **18**, 1890.

[9] F. Yang, M. Troncy, E. Francoeur, B. Vinet, P. Vinay, G. Czaika, G. Blaise, *Clin.Chem*, 1997, **43**, 657.

[10] P. Steinhoff, H. Kelm, *J. Chromatogr. B*, 1996, **685**, 348.

[11] M. H. Barley, K. J. Takeuchi, T. J. Meyer, *J. Am. Chem. Soc*, 1986, **108**, 5876.

[12] Y. Zhang, Y. Zhao, S. Yuan, H. Wang, C. He, *Sens. Actuators, B*, 2013, **185**, 602.

[13] C. Yu, J. Guo, H. Gu, *Electroanalysis*, 2010, **22**, 1005.

[14] N. I. Ikhsan, P. Rameshkumar, A. Pandikumar, M. M. Shahid, N. M. Huang, S. V. Kumar, H. N. Lim, *Talanta*, 2015, **144**, 908.

[15] G. Bharath, R. Madhu, S. M. Chen, V. Veeramani, D. Mangalaraj, N. Ponpandian, *J. Mater. Chem. A*, 2015, **3**, 15529.

[16] S. Sakthinathan, S. Kubendhiran, S. M. Chen, K. Manibalan, M. Govindasamy, P. Tamizhdurai, S. Tung Huang, *Electroanalysis*, 2016 , **28**, 1.

[17] A. Reina, X. Jia, J. Ho, D. Nezich, H. Son, V. Bulovic, M. S. Dresselhaus, J. Kong, *Nano Lett*, 2009, **9**, 30.

[18] S. Stankovich, D. A. Dikin, R. D. Piner, K. A. Kohlhaas, A. Kleinhammes, Y. Jia, Y. Wu, S. B. T. Nguyen, R. S. Ruoff, *Carbon*, 2007, **45**, 1558.

[19] K. S. Subrahmanyam, L. S. Panchakarla, A. Govindaraj, C. N. R. Rao, *J. Phys. Chem. C*, 113, **11**, 2009.

[20] D. Du, P. Li, J. Ouyang, *ACS Appl. Mater. Interfaces*, 2015, **7**, 26952.

View Article Online
DOI: 10.1039/C6RA20580A

[21] S. Park, J. An, J. R. Potts, A. Velamakanni, S. Murali, R. S. Ruoff. *Carbon*, 2011, **49**, 3019.

[22] X. Fan, W. Peng, Y. Li, X. Li, S. Wang, G. Zhang, F. Zhang. *Adv. Mater*, 2008, **20**, 4490.

[23] N. A. Santos, S. S. Damasceno, P. H. M. D. Araujo, V. C. Marques, R. Rosenhaim, V. J. Fernandes, J. N. Queiroz, I. M. G. Santos, A. S. Maia, A. G. Souza, *Energy Fuels*, 2011, **25**, 4190.

[24] S. A. S. Sunaga, T. Taniguchi, H. Miyazaki, T. Nabeshima, *Inorg. Chem*, 2007, **46**, 2959.

[25] P. Souza, J. A. G. Vazquez, J. R. Masaguer, *Transition Met. Chem*, 1985, **10**, 410.

[26] Y. Elerman, M. Kabak, A. Elmali, *Z. Naturforsch. B Chem.Sci*, 2002, **57**, 651.

[27] X. Q. Ji, L. Cui, Y. H. Xu, J. Q. Liu, *Compos. Sci. Technol*, 2015, **106**, 25.

[28] N. An, F. H. Zhang, Z. A. Hu, Z. M. Li, L. Li, Y. Y. Yang, B. S. Guo, Z. Q. Lei, *RSC Advances*, 2015, **5**, 23942.

[29] W. S. Hummers, R. E. Offeman, *J. Am. Chem. Soc*, 1958, **80**, 1339

[30] I. Correia, S. Roy, C. P. Matos, S. Borovic, N. Butenko, I. Cavaco, F. Marques, J. Lorenzo, A. Rodríguez, V. Moreno, J. C. Pessoa, *J. Inorg. Biochem*, 2015, **147**, 134.

[31] P. A. N. Reddy, M. Nethaji, A. R. Chakravarty, *Eur. J. Inorg. Chem*. 2004, **7**, 1440.

[32] K. Nagaraj, S. Sakthinathan, S. Arunachalam, *J Iran Chem Soc*, 2015, **12**, 267.

[33] K. Nagaraj, S. Sakthinathan, S. Arunachalam, *J. Fluoresc*, 2014, **24**, 589.

[34] Z. Bo, X. Shuai, S. Mao, H. Yang, J. Qian, J. Chen, J. Yan, K. Cen, *Sci. Rep,* 2014, **4**, 4684, DOI: 10.1038/srep04684

[35] H. Gou, J. He, Z. Mo, X. Wei, R. Hu, Y. Wang, *RSC Adv*, 2015, **5**, 60638.

[36] M. M. Seanu, I. Georgescu, L. E. Bibire, G. Carj, *Catal. Commun*, 2014, **54**, 39.

[37] K. M. Parida, M. Sahoo, S. Singha, *J. Mol. Catal. A Chem*, 2010, 329, 7.

[38] C. Y. Lin, A. Balamurugan, Y. H. Lai, K. C. Ho, *Talanta*, 2010, **82**, 1905.

[39] G. Guidelli, F. Pergola, G. Raspi, *Anal Chem*, 1972, **44**, 745.

[40] V. Mani, B. Dinesh, S. M. Chen, R. Saraswathi, *Biosens. Bioelectron,* 2014, **53**, 420.

[41] A. Afhami, F. S. Felehgari, T. Madrakian, H. Ghaedi, *Biosens. Bioelectron*, 2014, **51**, 379.

[42] S. J. Li, G. Y. Zhao, R. X. Zhang, Y. L. Hou, L. Liu, H. Pang, *Microchim. Acta*, 2013, **180**, 821.

[43] V. Mani, A. P. Periasamy, S. M. Chen, *Electrochem. Commun*, 2012, **17**, 75.

View Article Online
DOI: 10.1039/C6RA20580A

[44] C. Yang, J. Xu, S. Hu, *J Solid State Electrochem*, 2007, **11**, 514.

[45] G. R. Xu, G. Xu, M. L. Xu, Z. Zhang, Y. Tian, H. N. Choi, W. Y. Lee, *Bull. Korean Chem. Soc*, 2012, **33**, 415.

[46] S. Palanisamy, B. Thirumalraj, S. M. Chen, *J. Electroanal. Chem*, 2016, **760**, 97.

[47] K. Zhao, H. Song, S. Zhuang, L. Dai, P. He, Y. Fang, *Electrochem. Commun*, 2007, **9**, 65.

[48] A. R. Marlinda, A. Pandikumar, N. Yusoff, N. M. Huang, H. N. Lim, *Microchim Acta*, 2015, **182**, 1113.

[49] L. Zhang, E. M. Yi, *Bioprocess Biosyst Eng*, 2009, **32**, 485.

[50] Y. Cui, C. Yang, W. Zeng, M. Oyama, W. Pu, J. Zhang, *Anal Sci*, 2007, **23**, 1421.

[51] L. Zhang, F. Yuan, X. Zhang, L. Yang, *Chem Cent J*, 2011, **5**, 75.

[52] P. Miao, M. Shen, L. Ning, G. Chen, Y. Yin, *Anal. Bioanal. Chem*, 2011, **399**, 2407.

[53] R. Madhu, V. Veeramani, S. M. Chen, *Sci. Rep*, 2041, **4**, 4679, DOI: 10.1038/srep04679.

[54] X. Luo, A. J. Killard, M. R. Smyth, *Chem. Eur. J*, 2007, **13**, 2138.

[55] W. Xue, L. Hui, W. Min, G. S. Li, Z. Yan, W. Q. Jiang, H. P. Gang, F. Y. Zhi, *Chin J Anal Chem*, 2013, **41**, 1232.

View Article Online
DOI: 10.1039/C6RA20580A

Figure captions,

Table 1 Comparison on the analytical performance of RGO/[Cu(sal-ala)(phen)] nanocomposite modified electrode with other reported sensor.

Table 2 Determination of nitrite in real samples using RGO/ [Cu(sal-ala) (phen)] nanocomposite modified electrode.

Scheme 1 Synthesis of [Cu(sal-ala)(phen)] inorganic complex.

Scheme 2 Schematic representation for the preparation of RGO/[Cu(sal-ala)(phen)] nanocomposite for nitrite sensor.

Figure 1 SEM images of (A) GO, (B) RGO, (C) GO/[Cu(sal-ala)(phen)], (D) RGO/[Cu(sal-ala)(phen)], (Inset C') [Cu(sal-ala)(phen)], (E & F) EDX spectrum of RGO/[Cu(sal-ala)(phen)] nanocomposite**.**

Figure 2 (A) Electrochemical impedance spectrum of (a) Bare GCE (b) GCE/RGO, (c) [Cu(sal-ala)(phen)], (d) GO/[Cu(sal-ala)(phen)] and (e) RGO/[Cu(sal-ala)(phen)] modified electrode in 0.1 M KCl containing 5 mM $[Fe(CN)_6]^{3-/4-}$. **(B)** UV-Vis spectroscopy analysis of (a) RGO, (b) [Cu(sal-ala)(phen)] and (c) RGO/[Cu(sal-ala)(phen)].

Figure 3 (A) X-ray diffraction studies of (a) RGO, (b) [Cu(sal-ala)(phen)], (c) RGO/[Cu(sal-ala)(phen)]. **(B)** FT-IR spectra of (a) RGO, (b) [Cu(sal-ala)(phen)], (c) RGO/[Cu(sal-ala)(phen)].

Figure 4 (A) Cyclic voltammetry of (a) RGO/[Cu(sal-ala)(phen)] nanocomposite modified electrode in absence of nitrite, (b) bare GCE, (c) GCE/GO, (d) GCE/[Cu(sal-ala)(phen)], (e) GCE/RGO, (f) GO/[Cu(sal-ala)(phen)] and (g) RGO/[Cu(sal-ala)(phen)] in 0.05 M PBS (pH 5) containing 200 μM nitrite at scan rate 50 mV s^1. **(B)** Cyclic voltammetry response of RGO/[Cu(sal-ala)(phen)] nanocomposite at different concentration of nitrite in 0.05 M PBS (pH 5) at scan rate 50 mV s^{-1}.

Figure 5 (A) Cyclic voltammetry response of RGO/[Cu(sal-ala)(phen)] nanocomposite modified GCE in 200 μM nitrite containing different pH solution (2, 3, 5, 7, 9 & 11) at the scan rate of 50 mV s^{-1}, **(5B)** calibration plot for pH vs I_p.

View Article Online
DOI: 10.1039/C6RA20580A

Figure 6 (A) Cyclic voltammetry response of the RGO/[Cu(sal-ala)(phen)] nanocomposite modified GCE in PBS containing 200 μM of nitrite at different scan rate. **(6B)** calibration plot of square root of scan rate Vs. peak current.

Figure 7 (A) Amperometric response for the oxidation of nitrite with different concentration in PBS (pH 5), E_{app} = 0.75 V. The calibration plot of peak current vs. nitrite concentration (low **(B)** & high **(C)**)

Figure 8 (A) Amperometric response of hydrazine at RGO/[Cu(sal-ala)(phen)] in the presence of 50 μM nitrite and 500 μM addition of different interferences (b) Br^-, (c) I^-, (d) Cl^-, (e) NO_3^-, (f) F^-, (g) Cu^{2+}, (h) Zn^{2+}, (i) Cr^{2+}, (j) Sr^{2+}, (k) K^+, (l) dopamine, (m) glucose, (n) fructose and (o) ascorbic acid. **(8B)** Stability studies of the RGO/[Cu(sal-ala)(phen)] nanocomposite modified electrode.

View Article Online
DOI: 10.1039/C6RA20580A

Table 1

Electrodes	Linear range (µM)	LOD[a] (µM)	References
RGO[b]/[Cu(Sal-ala)[c](phen)[d]]	0.05-4, 6-1000	0.019	This work
poly(methylene blue)/GCE[e]	2.0-5000	2	45
graphite/β –cyclodextrin	0.7-2150	0.26	46
Thionine modified aligned /CNT [f]	3-5000	1.12	47
RGO-ZnO[g]	10-8000	33	48
Hb[h]/ PCAuPs[i]/MWCNT[j]	3.6 -3.09	0. 96	49
AuNPS[k]/GCE	1-5000	2.4	50
CuO[l]/GCE	5-180	1.6	51
PtNPs[m]	10-1000	5	52
HAC[n]	1-127	70	53
PANI[o]conducting polymer	5-1400	0. 24	54
AuNP/Graphene/Chitosan	1-380	0.25	55

Abbreviation

[a] Limit of detection**,** [b] Reduced graphene oxide, [c] salicylalanine, [d] phenanthroline, [e] Glassy carbon electrode, [f] carbon nanotubes, [g] Zinc oxide, [h] Hemoglobin, [I] Positively charged gold nanoparticle, [j] Multiwalled carbon nanotubes, [k] Gold nanoparticles, [l] Copper oxide, [m] Platinum nano particles, [n] Heteroatom enriched porous carbon, [o] Polyaniline

Table 2

Samples	Added (µM)	Found (µM)	Recovery (%)	RSD[a] (%)
Tap water	10	9.56	95.6	3.2
River water	10	10.2	102	3.5
Sausage 1	10	10.6	106	3.1
Sausage 2	10	10.3	103	3.2

[a]Relative standard deviation of 3 individual measurements.

View Article Online
DOI: 10.1039/C6RA20580A

Scheme 1

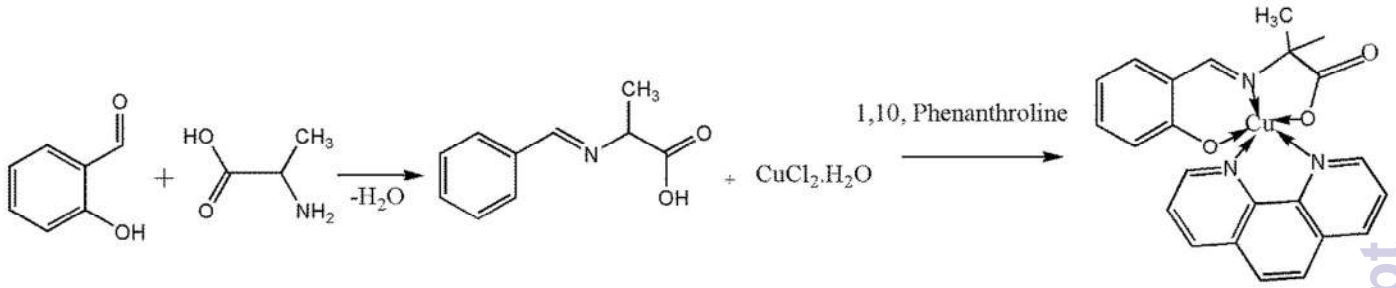

Scheme 2

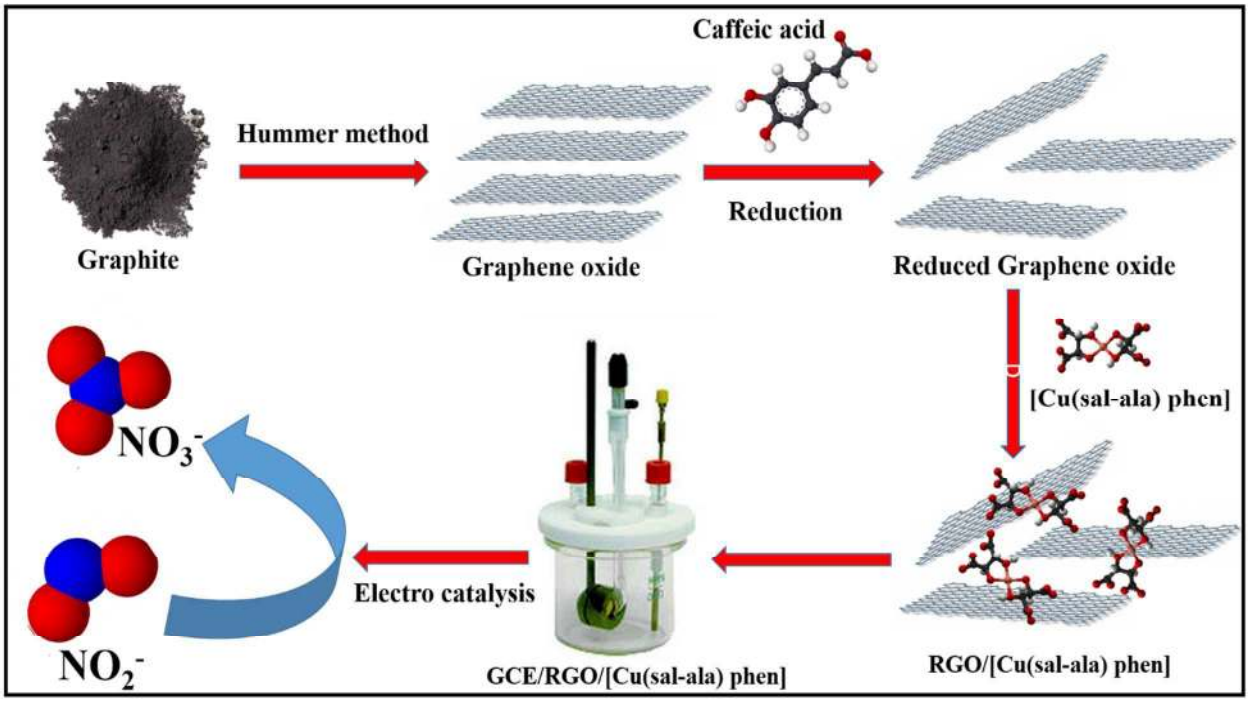

View Article Online
DOI: 10.1039/C6RA20580A

Figure 1

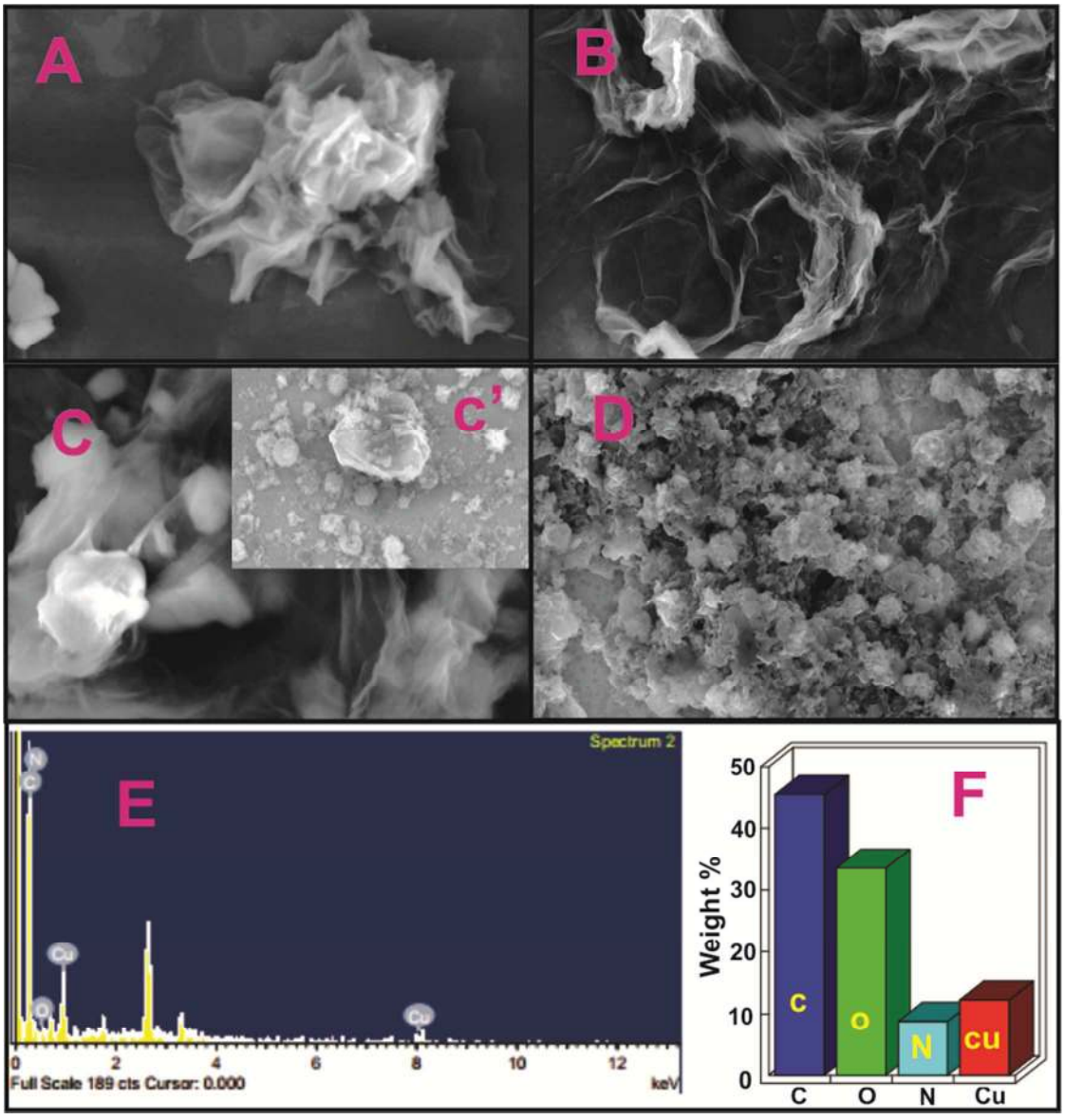

View Article Online
DOI: 10.1039/C6RA20580A

Figure 2

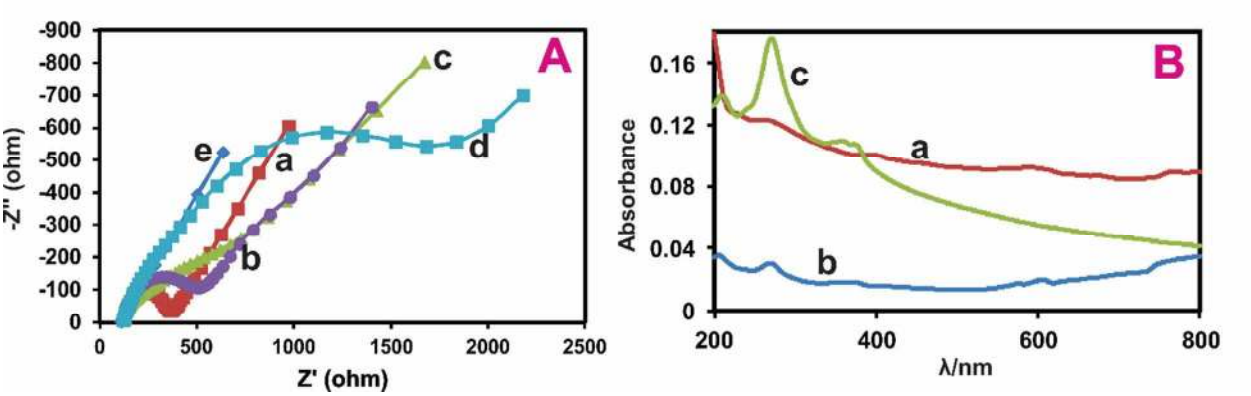

Figure 3

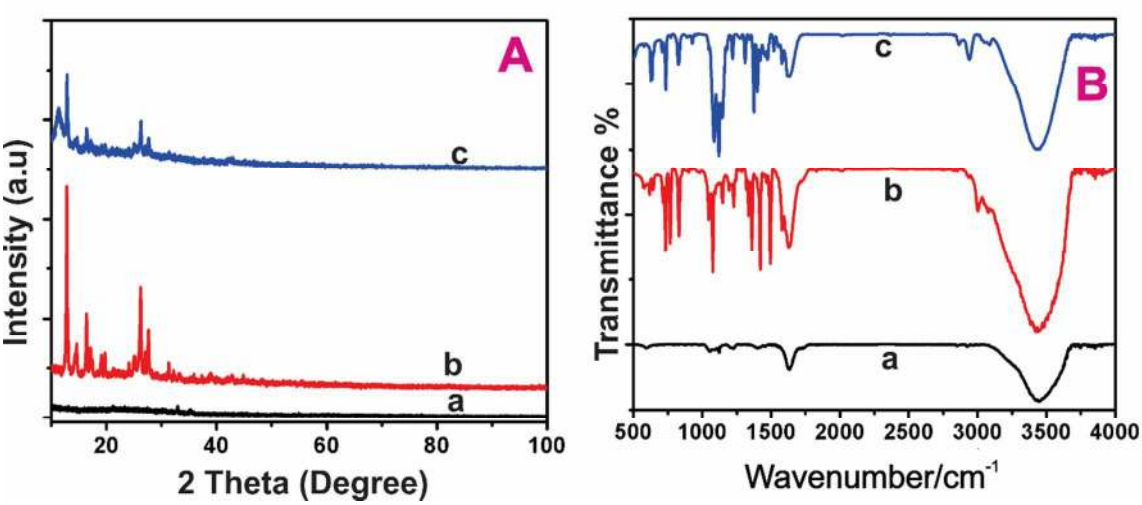

View Article Online
DOI: 10.1039/C6RA20580A

Figure 4

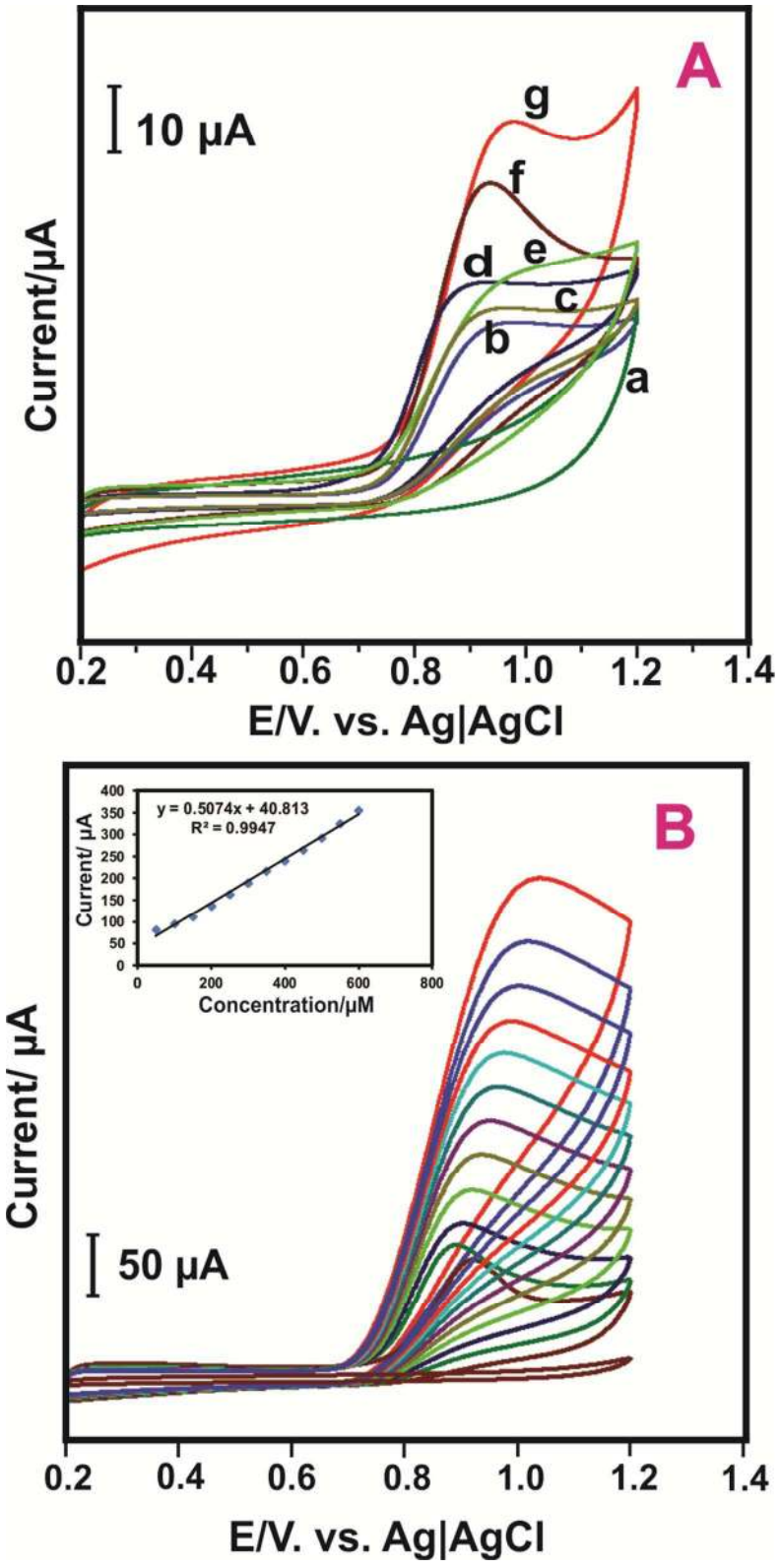

View Article Online
DOI: 10.1039/C6RA20580A

Figure 5

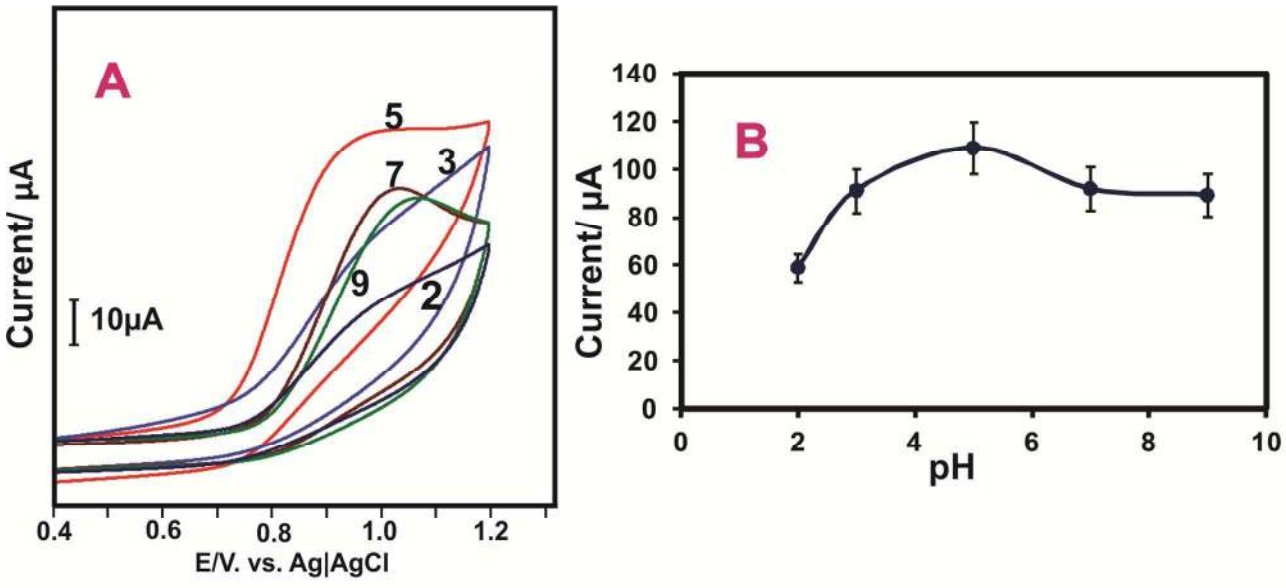

Figure 6

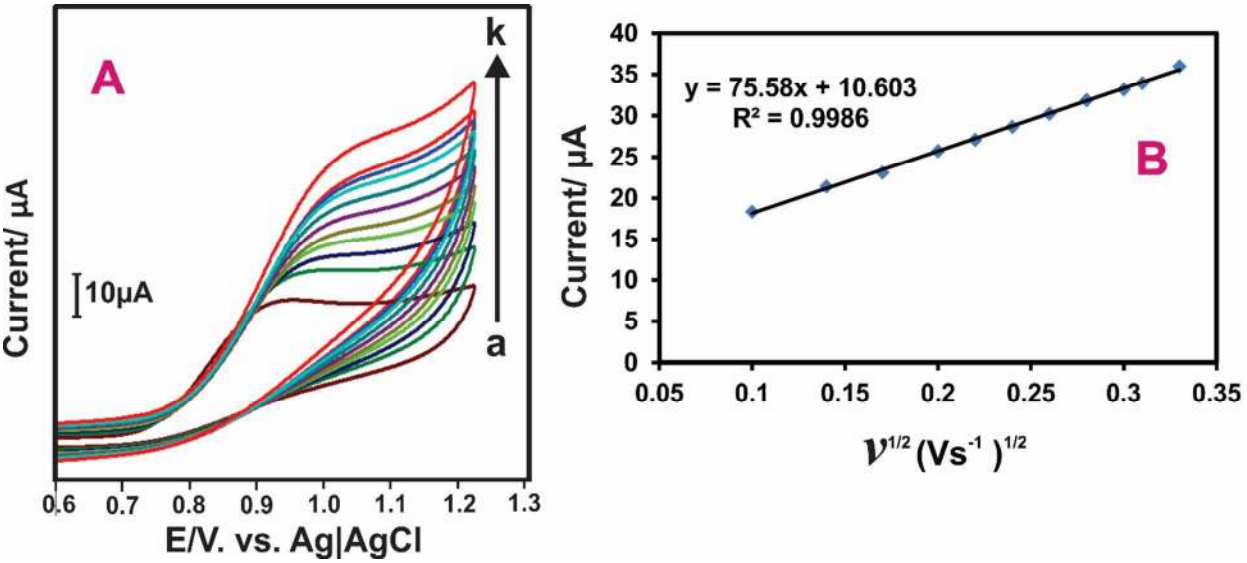

View Article Online
DOI: 10.1039/C6RA20580A

Figure 7

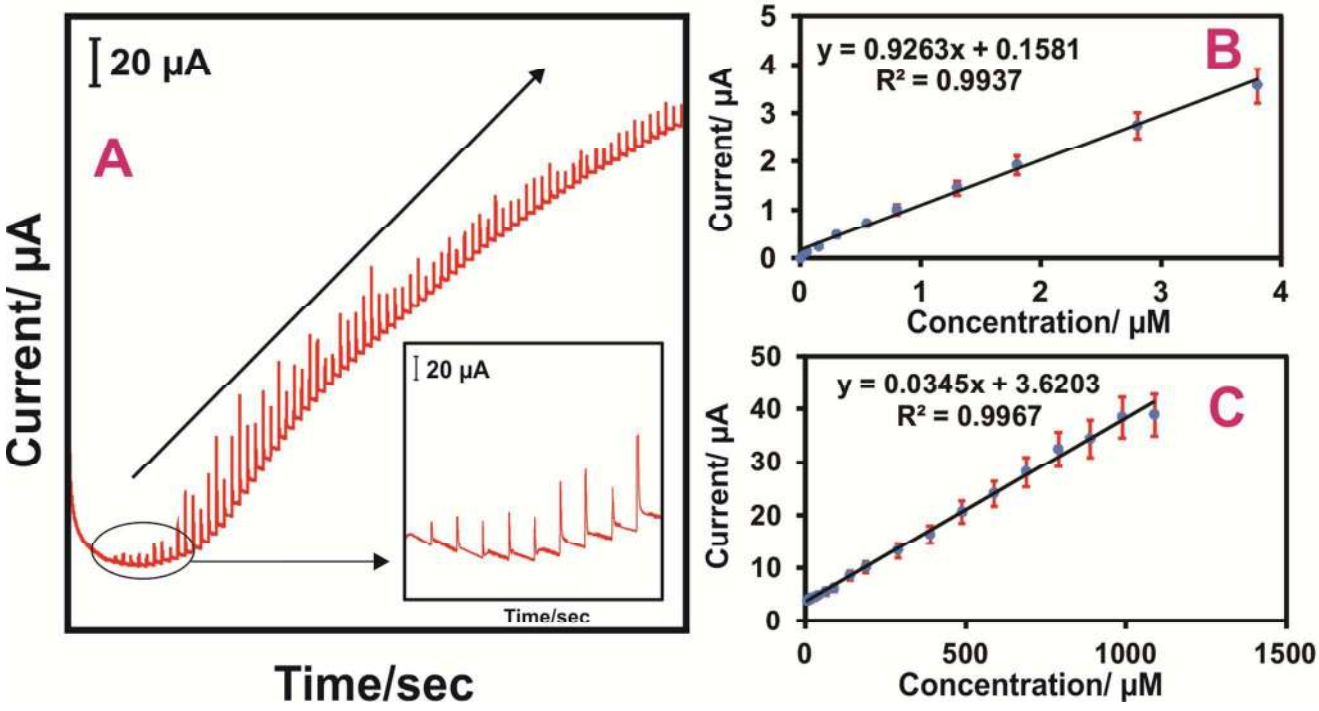

Figure 8

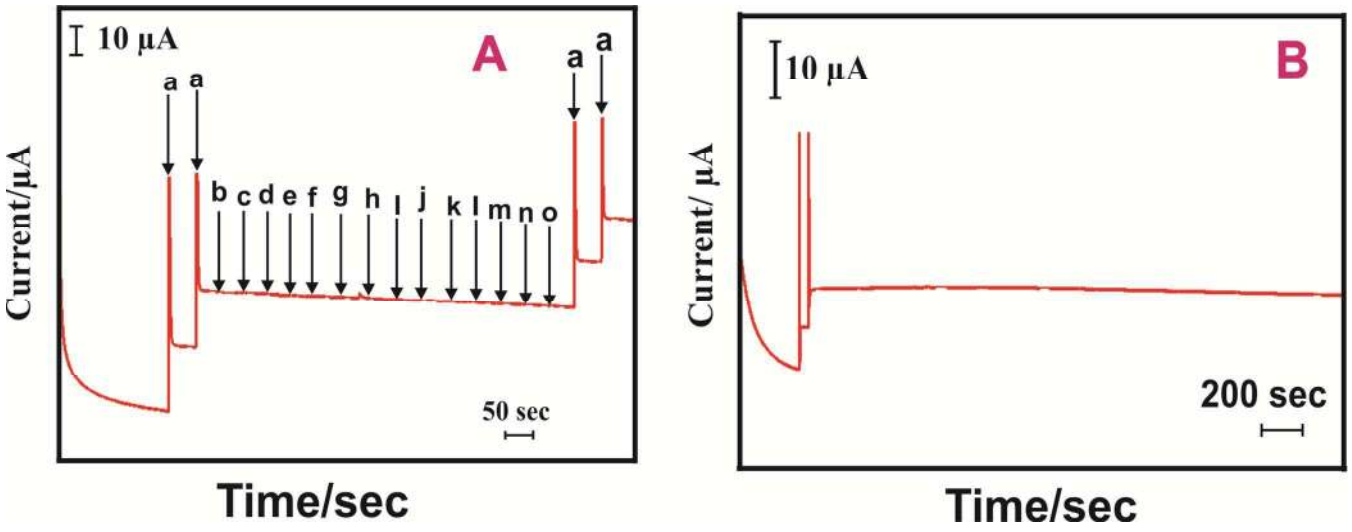

View Article Online
DOI: 10.1039/C6RA20580A

Graphical abstract,